JTTEE5 16:548–556
DOI: 10.1007/s11666-007-9069-9
1059-9630/$19.00 © ASM International

Laser Shock Flier Impact Simulation of Particle-Substrate Interactions in Cold Spray

S. Barradas, V. Guipont, R. Molins, M. Jeandin, M. Arrigoni, M. Boustie, C. Bolis, L. Berthe, and M. Ducos

(Submitted May 30, 2007; in revised form July 19, 2007)

Coating-substrate adhesion in cold spray is a paramount property, the mechanisms of which are not yet well elucidated. To go into these mechanisms, due to the intrinsic characteristics of the cold spray process (particle low-temperature and high velocity) direct observation and control of inflight particles and related phenomena cannot be done easily. For this reason, an experimental simulation of the particle-substrate reactions at the particle impingement was developed. This simulation is based on original flier impact experiments from laser shock acceleration. Relevant interaction phenomena were featured and studied as a function of shearing, plastic deformation, phase transformation primarily. These phenomena were shown to be similar to those involved in cold spray. This was ascertained by the study of the Cu-Al metallurgically reactive system using SEM, TEM, EPMA, and energy balance and diffusion calculations. This simulation could also be used to feed finite element modeling of cold spray and laser shock flier impact.

Keywords adhesion of TS coatings, coatings for gas turbine components, cold gas dynamic spraying, friction and wear, hydroxyapatite biomaterial, laser deposited materials, laser surface treatment, plasma spray forming, porosity of coatings, spray deposition

1. Introduction

One has no more to claim for a great potential of cold-gas dynamic-spray, i.e., the so-called ''cold spray,'' as the development of this spraying process can be considered as undeniable (Ref 1). However, despite the actual craze for cold spray, more than a flavor of mystery remains regarding the mechanisms involved in this coating process, primarily those related to (sprayed) particle-to-particle and particle-to-substrate adhesion. Except for the evidence of a critical particle velocity below which no adhesion could occur (Ref 2, 3) and that of the influence of particle and/or substrate plastic deformation (Ref 4, 5), one may say there is still little to say definitely in the field, due to needs in extensive research and development work. Most relevant are those based on the establishing of analogies between cold spray and either explosive welding (Ref 6-10) or dynamic compaction (Ref 11-13) as far as adhesion mechanisms are concerned. However, these studies dealt with observation, interpretation, and modeling of macroscopic solid-state phenomena such as the ejection of solid material (Ref 6-10). A transient liquid phase was sometimes predicted by modeling and/or assumed but never evidenced by direct observation. An exception is in a very recent work on cold spraying of zinc, i.e., a low-temperature material (Ref 6).

The present work therefore developed an innovative experimental simulation of particle-substrate simulation of particle-substrate interactions in cold spray coupled with thorough observation analysis of the corresponding interfaces. Significant advances were expected from laser shock flier impact experiments (Ref 14) for simulation and from interface metallurgical study at a fine scale using TEM for observation. The latter was already shown to be efficient to study cold spraying mechanisms at interfaces, e.g., oxidation (Ref 15).

The developed experimental simulation showed a high flexibility due to the use of laser shocks as exhibited in a pioneering work on laser shock cladding more than one decade ago by Dubrujeaud and Jeandin (Ref 16). This simulation was complemented by finite element (FE) modeling of cold-sprayed particle impinging on a substrate. These resulted in a discussion of interface phenomena in the light of a parallel microstructural study and consequently in setting criteria for cold spray coating adhesion.

2. Materials and Processes

The Cu-Al coating substrate system was selected for the study due to a high metallurgical reactivity between Al and Cu (Ref 17). The metallurgical state at the Cu-Al

S. Barradas, V. Guipont, and **M. Jeandin**, Centre des Matériaux/CNRS 7633, C2P-Competence Center for spray Processing, Mines Paris – ParisTech, Evry Cedex, France; **R. Molins**, Centre des Matériaux/CNRS 7633, Mines Paris – ParisTech, Evry Cedex, France; **M. Arrigoni,** and **M. Boustie**, LCD – Laboratoire de Combustion et de Détonique, CNRS UPR 9028, ENSMA, Futuroscope Chasseneuil Cedex, France; **C. Bolis** and **L. Berthe**, LALP – Laboratoire pour l'Application des Lasers de Puissance, UPR CNRS 1578, Arcueil Cedex, France; **M. Ducos**, Route d'Uchaux, Mornas, France. Contact e-mail: michel.jeandin@ensmp.fr.

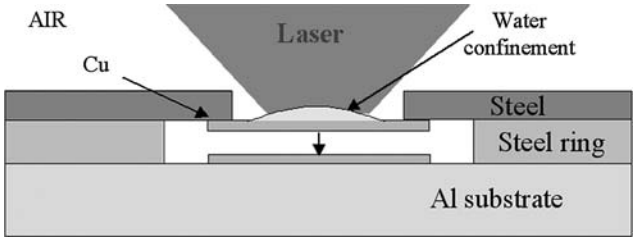

Fig. 1 Schematic illustration of the experimental set-up for laser shock flier impact experiments

interface could therefore be assumed to signify the ''story'' of the two materials when cold spraying Cu onto Al. The formation of intermetallics and the diffusion distance allowed to assess the temperature and time interaction between the materials.

2.1 Laser Shock Flier Impact Experiments

Laser shock flier impact experiments consisted in high-velocity cladding onto bulk Al, of a Cu foil, i.e., the flier, the acceleration of which was given by a laser shock (Fig. 1). The flier was made of a Cu foil (#CU000420 from GOODFELLOW, UK) of 25 μm in thickness. Prior to the laser shock, the flier was stuck to the steel sample holder horizontally due to a mere thin layer of grease, which left a distance to fly of 470 μm before reaching bulk Al (a platelet of 2 mm in thickness). For the shock, a one-shot laser beam from a QUANTEL PG28 Nd:YAG laser operating at 20 J during 20 ns focused on the Cu foil in a spot of 4 mm in diameter. A transparent medium to the laser, i.e., water, was deposited at the surface of the sample. It led to a confining of the shock on the sample and increased the shock pressure and time so that the beam-matter interaction was extended to 50 ns.

All the previously mentioned experimental conditions were determined through a preliminary study of the influence of relevant parameters such as the flying distance, the foil thickness, the dimensions and geometry of the various parts of the set-up, the laser beam energy distribution, and so on. These conditions were optimized to lead to a stabilized velocity of about 830 m s^{-1} (Fig. 2) which was typical of conventional cold-sprayed Cu particle velocity (Ref 18, 19). Foil velocity was measured by Doppler laser interferometry using a Velocity Interferometer System for Any Reflector (VISAR by Valyn Int., Albuquerque, USA) in preliminary flier impact experiments onto a material transparent to the VISAR laser beam (at 532 nm), i.e., PMMA (Poly Methyl Methacrylate) which replaced Al for this calibration (Fig. 2 insert).

2.2 Cold Spray

Commercial gas-atomized copper powder (MBC METAL POWDER Cu, $-22+5$ μm) was cold-sprayed onto mirror-polished Al substrates without any preheating. Conventional spraying conditions (Table 1) were applied using Linde/CGT cold spray facilities in Unterschleissheim/Germany (Kinetic 3000 M cold spray system with MOC type nozzle). A series of coatings of 300 μm in thickness were obtained.

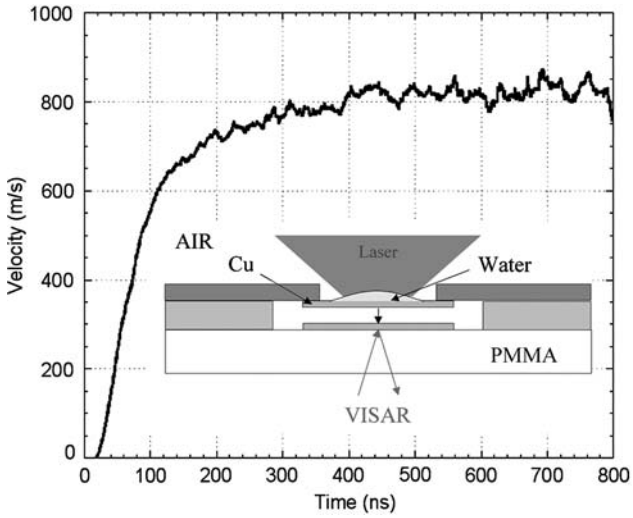

Fig. 2 Typical foil velocity profile vs. time and related experimental set-up (insert)

Table 1 Spraying conditions for cold-sprayed copper onto Al

Process gas	N_2
Pressure, MPa	2.8
Flow rate, l min^{-1}	1000
Temperature, °C	550
Carrier gas	N_2
Pressure, MPa	2.8
Flow rate, l min^{-1}	90
Powder feed rate, g min^{-1}	48
Spraying distance, mm	35

2.3 Microstructural Investigation

Specimens were studied by conventional optical microscopy, by scanning electron microscopy (SEM) using ''LEO 450VP'' and high-resolution ''ZEISS/GEMINI DSM 982'' microscopes, by electron probe micro-analysis (EPMA) using a ''CAMECA SX50'' microprobe, and by transmission electron microscopy (TEM) using a ''TECNAI F-20ST'' microscope equipped with analytical systems. STEM-EDX profiles with a nanometric probe size were performed to study interfaces. For this, thin foils were prepared by a focused ion beam (FIB) technique at FEI, Bristol/UK.

3. Laser Shock Flier Impact Experiments

3.1 Numerical Simulation of Dynamic Cladding

Three-dimensional calculations using ''RADIOSS®'' (licensed by ''Mecalog,'' Antony/France), i.e., an explicit FE code in a Lagrangian coordinate mode were performed. Foil and substrate material behaviors were described by a ''Johnson-Cook''-typed Law to simulate the

temperature increase due to deformation as a function of deformation rate. This modeling was considered as the most suitable for dynamic cladding similarly to explosive welding (Ref 20). The basic expression of the Law was:

$$\sigma_{eq} = (A + B\varepsilon_p^n)\left(1 + C\ln\frac{\dot{\varepsilon}_p}{\dot{\varepsilon}_{p0}}\right)\left(1 - \left(\frac{T - T_{init}}{T_{fus} - T_{init}}\right)^m\right) \quad \text{(Eq 1)}$$

with the dynamic properties:

σ_{eq}	Von Mises equivalent stress
A	Yield stress (Ref 21)
B	Hardening modulus (Ref 21)
ε_p (ε_{po})	Equivalent plastic deformation (initial value)
n	Hardening exponent (Ref 21)
C and m	Constants (Ref 21)
T (To)	Temperature (initial value)
T_{Fus}	Fusion temperature

Thorough preliminary studies on mesh size were carried out, though it is not detailed here. A thickness of 200 μm, i.e., higher than that of the actual experiments was tested in the modeling to increase the stress levels due to cladding and to exhibit better the impact stages during laser shock filer impact experiments. Calculations showed first that the center of the foil—which corresponded to the (laser shock) loading area—impinged on the substrate ahead of the rim. This resulted in oblique shock waves within the foil which led to tensile stresses at the foil-substrate interface. These stresses were generated first at the impact center, which provoked debonding of the foil (Fig. 3).

3.2 Interface Microstructure

Except for central debonding, as predicted by modeling (see section 3.1), which can be considered as non-relevant in this section, the Cu-Al interface obtained by flier impact experiments showed two combined microstructural features. The one was morphological, the other was metallurgical, Fig. 4. The morphological feature consisted of a typical wavy profile, the wavelength of which increased with the distance from the center of the impact. In addition, the orientation of the wave obliqueness changed when passing through this same center to result in a symmetrical profile. The metallurgical feature consisted of the presence of intermetallics, the amount of which was all the higher as approaching the center. The profile wavelength and intermetallic content were therefore closely-linked parameters.

Debonding at the center of the impact (Fig. 4f) can be explained by the tensile stress phenomena, which was simulated in section 3.1.

WDS (Wavelength Dispersive Spectrometry) using E.P.M.A. (Fig. 4g) showed η_2-AlCu and θ-Al_2Cu intermetallics. However, Al-Al_2Cu eutectic phase should exist but could not be detected due to a size and/or a content which did not meet the resolution of EPMA. In absence of information in the literature about the dynamic formation of (Al, Cu) intermetallics, the equilibrium diagram was used as a reference for metallurgical interpretations in this study.

4. Modeling of High-Velocity Impact in Cold Spray

Plastic deformation and related temperature increase of Cu and Al in cold spray were studied from a simulation of aspherical particle impinging on a flat substrate. FE calculations using "RADIOSS®" with the same assumptions and approach to the model as those already described in section 3.1 were carried out. The meshing was made of prismatic and parallelepipedic cells for the particle and the substrate, respectively. The particle velocity, particle diameter, and thickness of the substrate were 800 m s^{-1}, 15 μm and 2 mm respectively. Cooling and

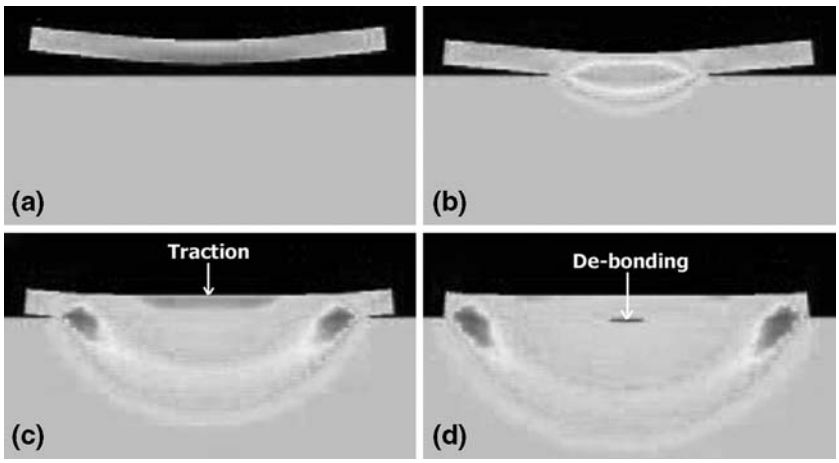

Fig. 3 Evolution of pressure at the flier impact, compression in dark gray (red in color printing) at the rim, tensile in light gray (blue in color printing) at the center

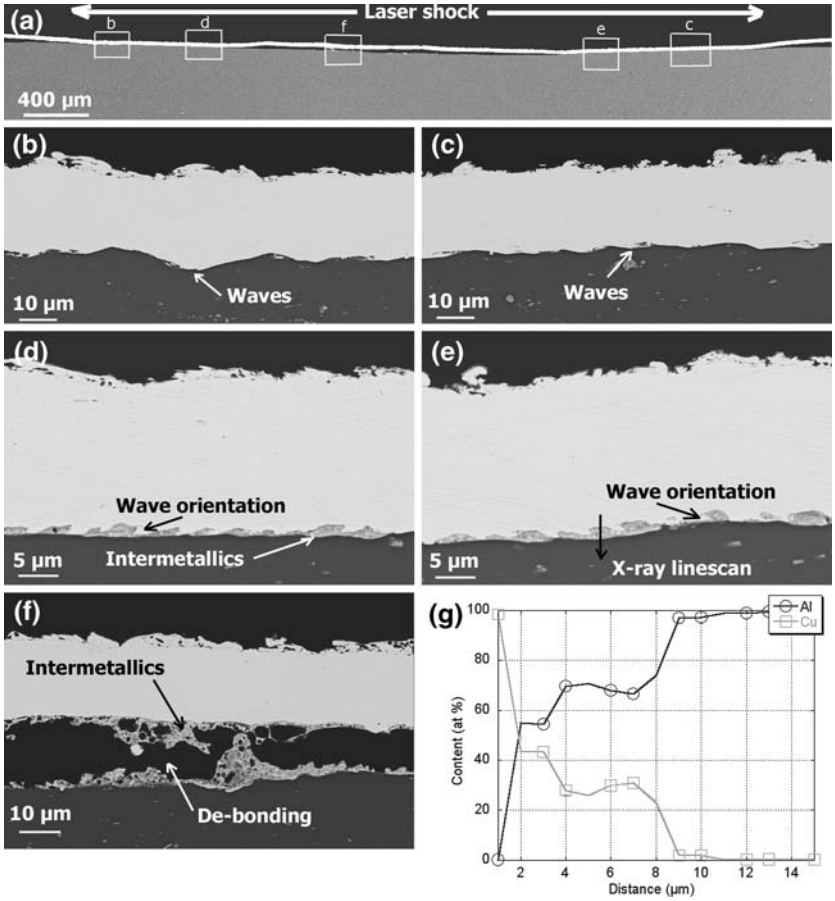

Fig. 4 Cross-section SEM micrographs of a 25 mm Cu foil onto Al after a laser shock flier experiment and typical WDS x-ray profiles

thermal conduction could not be studied from this simulation which assumed adiabatic conditions (Fig. 5).

Calculations led to the determining of the interaction time between Cu and Al, which was found to be equal to 20 ns. At this time from the first contact between Cu and Al, the Cu particle rebounded from the substrate, which defined the interaction time as established conventionally. Incidentally, the rebound was not due to shock wave reflection from neither the particle surface nor the substrate as shown in a parallel modeling study (Ref 22). This could be assumed to result from oblique shock waves which could generate tensile stresses, as shown in section 3.1.

As for temperature, numerical simulation showed that melting of Al, Cu, and Cu_2O could occur. There melting temperature are 660, 1083 and 1230 °C respectively. The alumina (Al_2O_3) could not melt for its melting temperature is about 2320 K. Moreover, temperature was all the higher as the material underwent the greater friction (i.e., primarily at the periphery of the Cu particle and Al substrate) and greater deformation (at the bottom of the impact area for the Al substrate) (Fig. 6). The center of the impact area of the substrate is, however, heated for a longer period than the periphery of the impact zone.

One may note that the trefoil-like distribution of temperature and the asymmetry resulted from numerical artifacts due to the use of parallelepipeds for meshing and to meshing mismatch during the collision, which, however, had no influence on the above-mentioned conclusions.

5. Cold-Sprayed Particle-Substrate Interface Microstructure

Interface general shape resulted from plastic deformation of Cu and Al and was in keeping with modeling results (see section 4 and Fig. 7).

Cu-Al interface showed α_2-$AlCu_4$, η_2-AlCu, and θ-Al_2Cu intermetallic phases, the amount and distribution of which depended on the location at the interface. Three types of interfaces could be determined (Fig. 8). The first type showed, α_2, η_2, and θ phases successively. No Al-Al_2Cu eutectic phase could be achieved. Al_2Cu crystallized in equiaxed nanograins of about 400 nm in average size. The second type was characterized by very fine AlCu and large Al-Al_2Cu eutectic areas and, as in type 1, $AlCu_4$ and Al_2Cu. The third type exhibited the same intermetallics that could form layers of 20 nm in thickness typically. Moreover, whatever the type of interface, oxygen (in a content of less than 15 wt.%), as a marker for diffusion, was detected through the whole interface width.

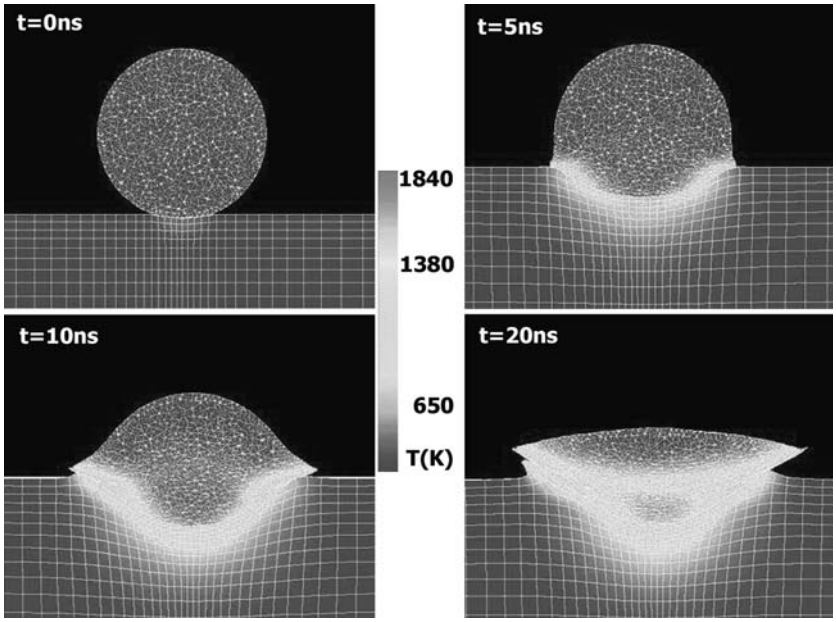

Fig. 5 Simulation of Cu particle (∅ 15 μm, $v = 800$ m s^{-1}) impingement on Al

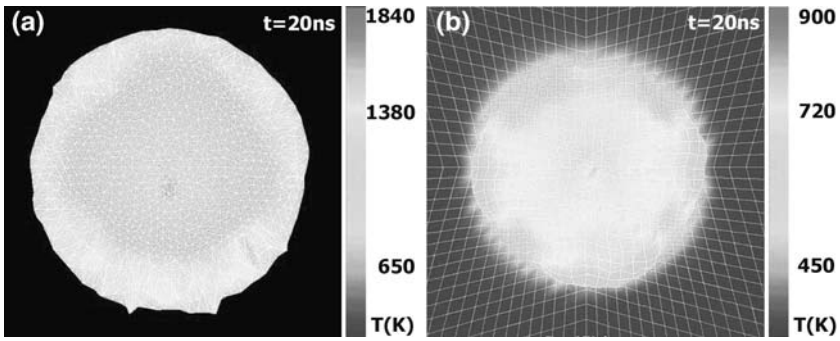

Fig. 6 Field of temperature at the end of the interaction, (a) for Cu (bottom view), (b) for Al (top view)

Type 1, which corresponded to the highest Cu-Al interaction, i.e., the largest diffusion depth, was located at the bottom of the particle impingement valley. This was in agreement with results from modeling (see section 4) which showed the higher substrate temperature in this region. The subsequent discussion (in section 6) will revert to this aspect.

6. Discussion

Both cold spray and laser shock flier impact experiments led to a coating-substrate interface which exhibited more or less intermetallic compounds of various types depending on the location along the interface. These formed from a liquid phase since modeling of particle impinging showed that temperature could rise above melting temperature at the Cu-Al interface (see section 4).

The aluminum oxide initially at the surface of the substrate may have dehydrate with the temperature increase at the interface. This could promote the Cu bonding to the ceramics. The alumina layer could have also cracked due to the mechanical effect of the particle impact, leaving the Cu and the Al in direct contact for liquid interdiffusion. As a consequence, the oxygen observed at the interface after impact (see section 5) may be explained by diffusion of the oxygen initially at the surface of the Cu powder and/or of the Al substrate.

Melting could also occur during laser shock flier experiments as ascertained by a rather rough analytical approach to the conversion of the kinetic energy to heat (computer modeling was not needed). In this approach, it was assumed that 90% of the total energy was used for deformation (Ref 20, 23) and that 80% of the latter resulted in heat (Ref 9, 23). Assuming also that a certain substrate and flier volume only underwent deformation and temperature increase, the kinetic-to-heat energy expression was:

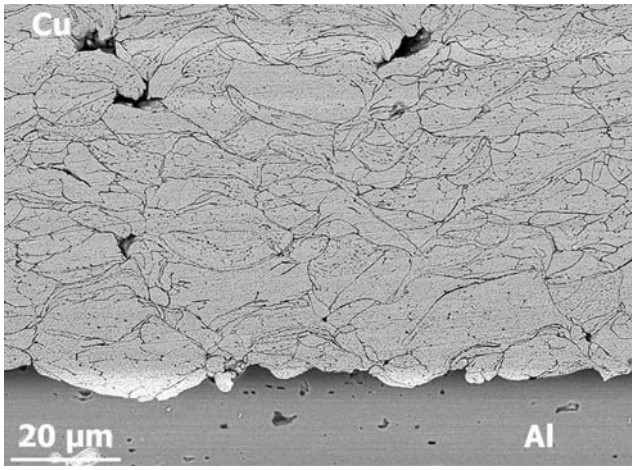

Fig. 7 Cross-section SEM micrograph of cold-sprayed Cu onto Al (after ''Keller'' etching)

$$(0.9 \times 0.8)\left[\frac{1}{2} m_{\mathrm{Part}} v_{\mathrm{Part}}^2\right] = \frac{\rho_{\mathrm{Al}}}{M_{\mathrm{Al}}} V_{\mathrm{Al}} \left[\int_{T_0}^{T} C_p^{\mathrm{Al}}(T)dt + L_{\mathrm{F}}^{\mathrm{Al}}\right] + \frac{\rho_{\mathrm{Cu}}}{M_{\mathrm{Cu}}} V_{\mathrm{Cu}} \left[\int_{T_0}^{T} C_p^{\mathrm{Cu}}(T)dt + L_F^{\mathrm{Cu}}\right] \quad \text{(Eq 2)}$$

where:

m_{part} Incident Cu particle mass
v_{part} Incident Cu particle velocity
V_{Al} Al volume involved in the transfer
V_{Cu} Cu volume involved in the transfer
ρ Density (2832−0.45 T for Al and 9191−0.89 T for Cu, in kg m^{-3})
M Molar mass (26.98 for Al and 63.54 for Cu in g mol^{-1})
C_P Molar heat capacity at a given pressure (as a function of temperature, from (Ref 24))
L_F Molar fusion latent heat (13,020 for Al and 10,470 for Cu, in J mol^{-1} (Ref 24))
T Temperature

For a 25 µm thick foil at a velocity of 830 m s^{-1} (i.e., the experimental conditions, see section 2.1), assuming the heat over 1 mm in thickness in both Al and Cu (Fig. 4d, e), temperature was calculated to reach about 5200 K from the Eq. 2. Even though this value might differ from the actual temperature due to starting assumptions, the order of magnitude of the result led to the conclusion that local energy was enough to provoke melting.

When therefore considering liquid-state diffusion in actual cold spray, the diffusion coefficient, D, could be determined using the ''Stokes-Einstein-Sutherland'' model (Ref 25, 26) for Cu atoms diffusing in liquid Al expressed by (Ref 27):

$$D = \frac{kT}{6\pi r \eta(T)} \quad \text{(Eq 3)}$$

where:

k Boltzmann's constant
T Temperature
r Diffusion particle radius (2.10^{-10} m for Cu (Ref 26, 27))
η Solvent (Al) viscosity

This led to a diffusion coefficient of about 10^{-8} m^2 s^{-1} at 1500 K. From the Fick's Law (Ref 28), in which

$$d_{\mathrm{diff}} = \sqrt{D \cdot t_{\mathrm{Diff}}}, \quad \text{(Eq 4)}$$

the diffusion distance, d_{diff}, was inferred to be therefore about 15 nm, since t_{diff} was known to be equal to 20 ns from the modeling study (see section 4).

This calculated diffusion distance did correspond to the width of the intermetallic area, which was observed experimentally (see section 5). This ascertained the formation of the intermetallic compounds through transient melting at the coating-substrate interface. Transient melting was therefore featured as a major mechanism which might govern interface properties in cold-sprayed materials. As a striking example of this, one may say that intermetallics can be beneficial to cold-sprayed coating-substrate adhesion due to a sort of spot welding effect at the interface but detrimental to plasma-sprayed coating-substrate adhesion due to conventional hard-phase embrittlement effect (Ref 29).

Incidentally, assuming solid-state diffusion only in cold spray would have led to a diffusion distance of 0.15 nm, which was not at all in agreement with observation.

A similar approach to liquid-phase diffusion and related calculations were carried out for laser flier experiments. These led to a diffusion distance that underestimated the typical experimental width of about 2 µm (see section 3.2) due to the neglecting of the influence of pressure (Ref 30). However, this result was considered to be significant enough to ascertain a transient melting mechanism since solid-state assumption would have been all the more excluded as the calculated distance was much lower.

Laser shock flier experiments resulted in laser shock cladding which can be discussed in an analogy with conventional explosive welding. The process is based on a high-velocity locally oblique impact where the velocity of the collision part (v_C) can be expressed as a function of the collision angle, β, and the velocity of the foil, v_F, by the following equation (Fig. 9).

$$v_C = \frac{v_F}{\tan \beta} \quad \text{(Eq 5)}$$

The various interface interaction phenomena involved in laser flier experiments can be exhibited in a collision (angle, velocity) diagram which had been designed formerly for conventional explosive welding (Fig. 10) (Ref 31). This diagram showed the predominance areas for welding with melting and/or wave formation.

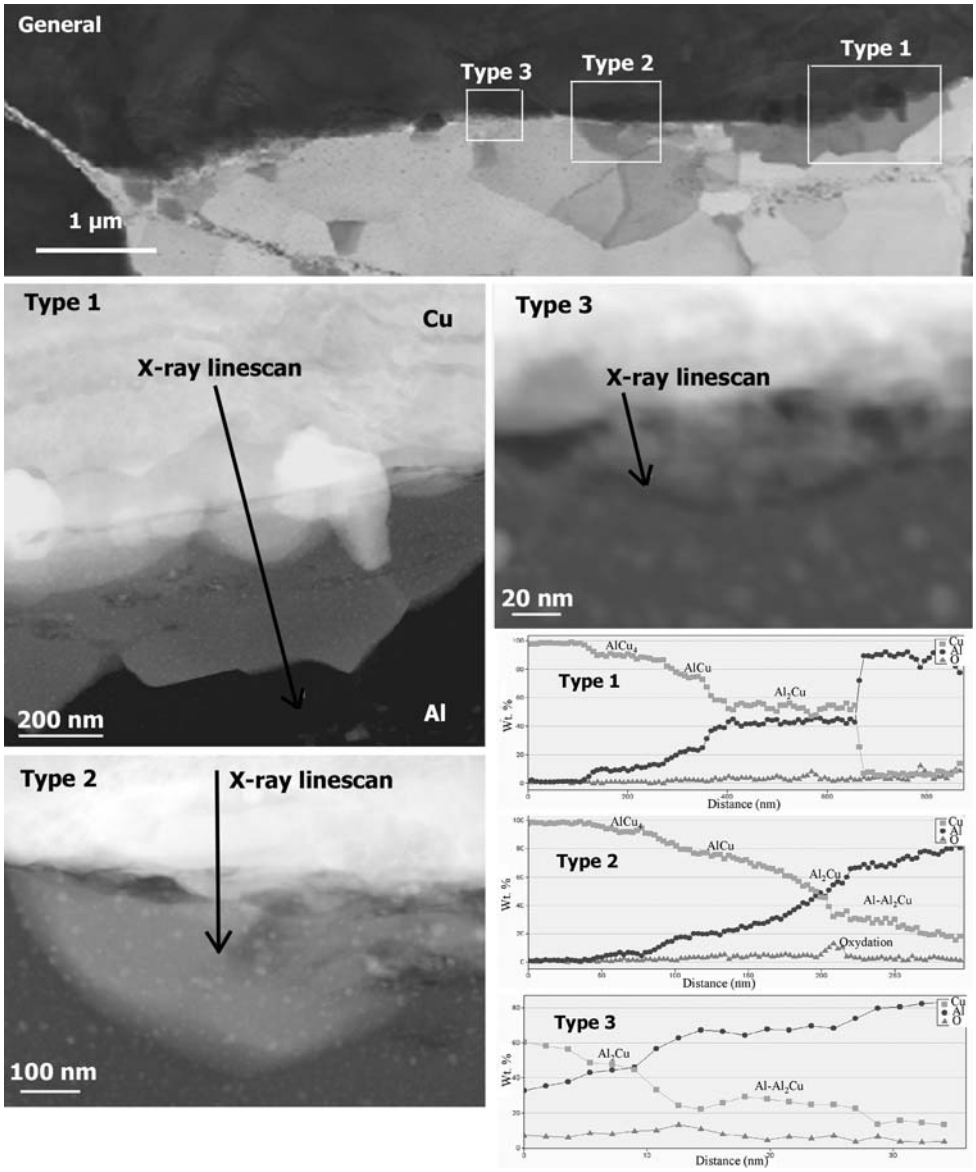

Fig. 8 TEM micrographs of cold spray Cu-Al interfaces and corresponding x-ray profiles. General view (bright field image) and 3 types of interfaces (HAADF-High Angle Annular Dark Field images)

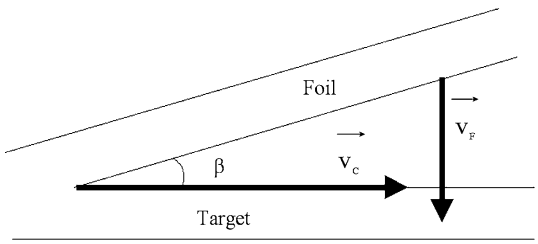

Fig. 9 Impact area configuration in the cladding of a foil

The impact center of the flier corresponds to high angles and high velocities related to interface melting and formation of intermetallic compounds. On the other hand, at the foil rims, i.e., for lower angles but higher velocities, waves do exist but result from solid-state deformation only without therefore any intermetallic. Intermediate areas show waves the frequency of which is all the higher as the liquid phase amount is higher (i.e., when approaching the impact center).

Cold spray, due to the spherical shape of the particle corresponds to higher collision angles compared to laser shock cladding of a foil. Particle-substrate interaction in cold spray is therefore similar to that of a foil at the center of the impact in a laser flier experiment (Fig. 10). Basically, there is no generation of waves even though some small waves could be observed locally at cold-sprayed interfaces (Fig. 11). However, these were not numerous and attributed to local deformation instabilities.

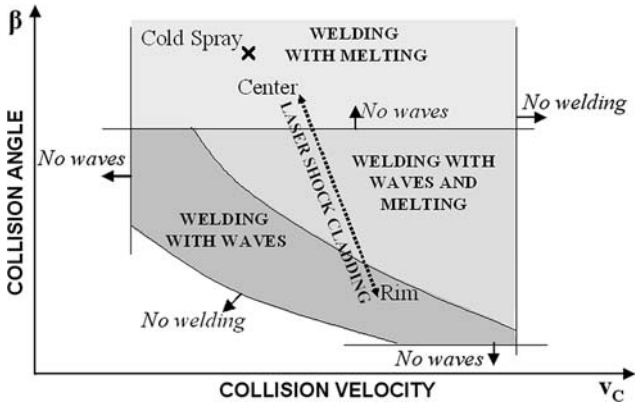

Fig. 10 Interface phenomenological diagram, after (Ref 31)

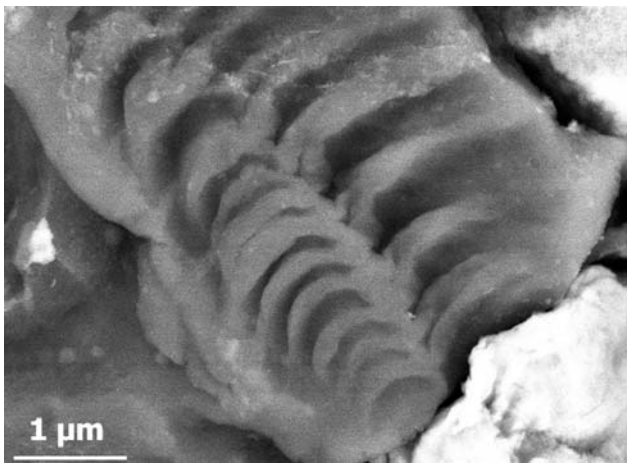

Fig. 11 SEM top view of the Al substrate surface after the removal of cold-sprayed Cu coating

7. Conclusion

Coating-substrate interface was shown to involve complex morphological and metallurgical phenomena which can be claimed to govern macroscopic properties, primarily coating-substrate adhesion. These phenomena could be featured through deliberate selection of a reactive coating-substrate system, i.e., copper-aluminum, for the study. Using this system, intermetallics, i.e., $AlCu_4$, Al_4Cu_9, AlCu, Al_2Cu, and Al-Al_2Cu eutectics, were exhibited to act as suitable and efficient markers of basic mechanisms involved in cold spray. The most prominent of these mechanisms was that of transient melting at the coating-substrate interface which formed from the cold-sprayed particle impact. Transient melting was ascertained by liquid-state diffusion calculations in an approach to the achievement of intermetallics combined to the modeling of the particle impinging on the substrate.

Relationships between the amount, nature and distribution of intermetallics and interface morphology and, one may assume, strength were established. These resulted from a thorough TEM investigation into interfaces combined to the development of an innovative experimental simulation of the cladding/ impinging of a material onto a substrate. This simulation was based on the use of controlled laser shock acceleration of a foil which could simulate a cold-sprayed particle, in so-called ''laser shock flier impact experiments.'' The work demonstrated the feasibility of reproducing metallurgical and morphological interface mechanisms involved in cold spray through this experimental simulation. These mechanisms were discussed in the light of those in one may term a parent process for cold spray and laser-shock cladding, i.e., explosive welding. Key strengths of the laser shock-based experimental simulation rest on the magnification and control of the material phenomena in addition to a low cost and high reproducibility. This simulation can be therefore expected to become a powerful tool for optimizing processing conditions in cold spray.

Above-mentioned conclusions featured the role of local phenomena, which suggests the actual existence of a narrow window for processing conditions for some materials (which could be given as a function of collision velocity and angle). One may therefore also expect for the developed simulation to be a tool to study the extension of cold spray to materials other than those conventionally said to be suitable for the process, e.g., ductile materials. Since local phenomena were shown to play a major role, future work should deal with the development of local testing of mechanical properties. First steps towards this were made in the same framework with the development of Laser Shock Adhesion Testing (LASAT) (Ref 32).

Acknowledgments

This work was supported by French Ministry of Education and Research (MENRT), which is gratefully acknowledged. The authors would like to thank Mr. G. Barbezat from SULZER METCO (Wohlen, Suisse), Mrs. F. Le Strat from GIE REGIENOV (Guyancourt,France), Mrs. B. Dumont from KME/TREFIMETAUX (Sérifontaine, France), and Mr. R. Gole form APS PLETECH (Marne la Vallée, France) for financial support and helpful discussions. Many thanks also to Mrs. N. De Dave, Mr. G. Frot, and Mrs O. Adam from the ''Ecole des Mines de Paris'' for technical assistance. The Linde and CGT companies (Germany) is also greatly acknowledged for the supplying of cold sprayed coupons and consumables.

References

1. F. Gärtner, H. Kreye, T. Schmidt, T. Stoltenhoff, and H. Assadi, Bonding Mechanisms and Applications of Cold Spraying, *Surface Modification Technologies 18*, T.S. Sudarshan, M. Jeandin, and J.J. Stiglich, Eds., Nov 15-17, 2004 (Dijon), IoM, London, UK, 2006, p 35-43
2. R.C. McCune, A.N. Papyrin, J.N. Hall, W.L. Riggs, and P.H. Zajchowski, An Exploration of the Cold Gas-Dynamic Spray Method for Several Materials Systems, *Advances in Thermal Spray Science & Technology*, C.C. Berndt and S. Sampath, Eds., Sep 11-15, 1995 (Houston, TX), ASM International, 1995, p 1-5

3. S.V. Klinkov, V.F. Kosarev, and M. Rein, Cold Spray Deposition: Significance of Particle Impact Phenomena, *Aerospace Sci. Technol.*, 2005, **9**, p 582-591
4. H. Fukanuma and N. Ohno, A Study of Adhesive Strength of Cold Spray Coatings. *Thermal Spray 2004: Advances in Technology and Application*, ASM International, May 10-12, 2004 (Osaka, Japan), 6 p
5. T.H. Van Steenkiste, J.R. Smith, R.E. Teets, J.J. Moleski, D.W. Gorkiewicz, R.P. Tison, D.R. Marantz, K.A. Kowalsky, W.L. Riggs, P.H. Zajchowski, B. Pilsner, R.C. McCune, and K.J. Barnett, Kinetic Spray Coatings, *Surf. Coat. Technol.*, 1999, **111**, p 62-71
6. Chang-Jiu Li, Wen-Ya Li, and Xi'an, Impact Fusion Phenomenon during Cold Spraying of Zinc, op. cit. ref. 4, 6 p
7. M. Grujicic, C.L. Zhao, W.S. DeRosset, and D. Helfritch, Adiabatic Shear Instability Based Mechanism for Particles/Substrate Bonding in the Cold-Gas Dynamic-Spray Process, *Mater. Design*, 2004, **25**, p 681-688
8. M. Grujicic, J.R. Saylor, D.E. Beasley, W.S. DeRosset, and D. Helfritch, Computational Analysis of the Interfacial Bonding between Feed-Powder Particles and the Substrate in the Cold-Gas Dynamic-Spray Process, *Appl. Surf. Sci.*, 2003, **219**, p 211-227
9. H. Assadi, F. Gärtner, T. Stoltenhoff, and H. Kreye, Bonding Mechanism in Cold Gas Spraying, *Acta Mater.*, 2003, **51**, p 4379-4394
10. R.C. Dykhuizen, M.F. Smith, D.L. Gilmore, R.A. Neiser, X. Jiang, and S. Sampath, Impact of High Velocity Cold Spray Particles, *J. Therm. Spray Technol.*, 1999, **8**, p 559-564
11. T. Schmidt, F. Gärtner, and H. Kreye, Bonding Mechanisms and Critical Impact Velocity in the Cold Spray Process, *Cold Spray 2004: An Emerging Spray Coating Technology*, ASM International, 2004, CD-Rom
12. T. Schmidt, F. Gärtner, and H. Kreye, High Strain Rate Deformation Phenomena in Explosive Powder Compaction and Cold Gas Spraying, *Thermal Spray 2003, Advancing the Science & Applying the Technology*, B.R. Marple and C. Moreau, Eds., May 5-8, 2003 (Orlando, FL), ASM International, 2003, p 9-18
13. T. Schmidt, F. Gärtner, H. Assadi, and H. Kreye, Development of a Generalized Parameter Window for Cold Spray Deposition, *Acta Mater.*, 2006, **54**, p 729-742
14. M. Boustie, M. Arrigoni, J. Jerome, L. Berthe, C. Bolis, M. Jeandin, and S. Barradas, The Flier Laser Shock Adhesion Test (F-LASAT) as an Extension of the LASAT Test for Coating/Substrate Systems Thickness above the Millimetric Range, op. cit. ref. 1, p 271-275
15. S. Barradas, R. Molins, M. Jeandin, M. Arrigoni, M. Boustie, C. Bolis, L. Berthe, and M. Ducos, Application of Laser Shock Adhesion Testing (LASAT) to the Study of the Interlamellar Strength and Coating-Substrate Adhesion in Cold-Sprayed Coating Systems, *Surf. Coat. Technol.*, 2005, **197**, p 18-27
16. B. Dubrujeaud and M. Jeandin, Cladding by Laser Shock Processing, *J. Mater. Sci. Lett.*, 1994, **13**, p 773-775
17. F.A. Calvo, A. Urena, J.M.G Salazar, and F. Molleda, Special Features of the Formation of the Diffusion Bonded Joints between Copper and Aluminium, *J. Mater. Sci.*, 1988, **23**, p 2273-2280
18. T. Stoltenhoff, H. Kreye, and H.J. Richter, An Analysis of the Cold Spray Process and its Coatings, *J. Therm. Spray Technol.*, 2002, **11**, p 542-550
19. H. Kreye, T. Schmidt, F. Gärtner, and T. Stoltenhoff, The Cold Spray Process and its Optimization, *ITSC 2006: Building on 100 years of Success*, B.R. Marple, Ed., May 15-18, 2006, (Seattle, Washington) 2006
20. A.A. Akbari Mousavi, S.J. Burley, and S.T.S. Al-Hassani, Simulation of Explosive Welding Using the Williamsburg Equation of State to Model Low Detonation Velocity Explosives, *Int. J. Impact Eng.*, 2005, **31**, p 719-734
21. G.R. Johnson and W.H. Cook, A Constitutive Model and Data for Metals Subjected to Large Strains, High Strain Rates and High Temperatures, *7th Int. Symp. on Ballistics*, 1983, (The Hague), p 541-547
22. C. Bolis, L. Berthe, M. Boustie, M. Arrigoni, H.L. He, M. Jeandin, and S. Barradas, Visar Pull-Back Signals as a Diagnostics for the Laser Adherence Test Applied to Copper Coating on Aluminium Substrate, AIP Conf. Proc, *Shock Compression of Condensed Matter*, **706**, 2004, p 1373-1376
23. I.M. Hutchings, A Model for the Erosion of Metals by Spherical Particles at Normal Incidence, *Wear*, 1981, **70**, p 269-281
24. "Smithells Metals Reference Book," E.A. Brandes, Ed., G.B. Brook, Butterworth, 1992
25. C. Jayaram, R. Ravi, and R.P. Chhabra, Calculation of Self-diffusion Coefficients in Liquid Metals Based on Hard Sphere Diameters Estimated from Viscosity Data, *Chem. Phys. Lett.*, 2001, **341**, p 179-184
26. A.S. Chauhan, R. Ravi, and R.P. Chhabra, Self-diffusion in Liquid Metals, *Chem. Phys.*, 2000, **252**, p 227-236
27. H.J.V. Tyrrell, Diffusion and Viscosity in the Liquid Phase, *Sci. Prog.*, 1981, **67**, p 271-293
28. Y. Adda and J. Philibert, "La Diffusion dans les Solides," PUF, (Paris), Vol 2, 1966, (in French)
29. S. Barradas, F. Borit, V. Guipont, M. Jeandin et al., Study of the Role of (Cu,Al) Intermetallics on Adhesion of Copper Plasma-sprayed on to Aluminum Using Laser Shock Adhesion Testing (LASAT), *International Thermal Spray Conference*, E. Lugscheider and C.C. Berndt, Eds., March 4-6, 2002 (Essen, Germany), DVS Deutscher Verband für Schweiben, 2002, p 592-597
30. V.V. Sobolev, J.M. Guilemany, J. Nutting, and J.R. Miquel, Development of Substrate-coating Adhesion in Thermal Spraying, *Int. Mater. Rev.*, 1997, **42**, p 117-136
31. T.Z. Blazynski, *Explosive Welding, Forming and Compaction*, Chapter 6, Applied Sci. Publishers, 1989, p 189-210
32. M. Ducos, B. Bossuat, H. Walaszek, S. Barradas, M. Jeandin, M. Arrigoni, M. Boustie, C. Bolis, and L. Berthe, Non Destructive Adhesion Testing of Plasma-sprayed Coatings Using Ultrasounds and Laser Shocks, op. cit. ref. 4, 6 p